Supplementary Materials:

Supplementary Figure 1, related to Figure 2:

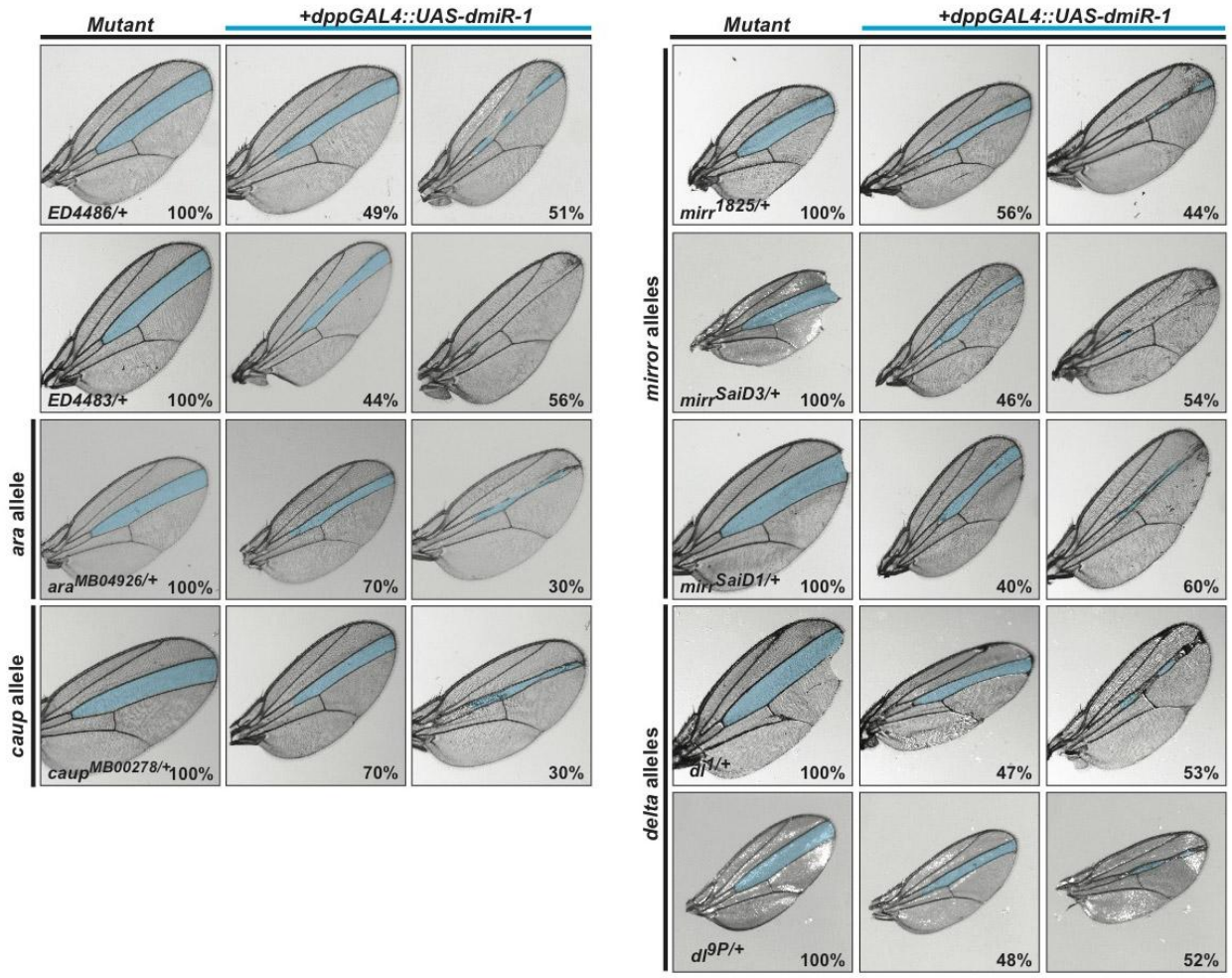

Fig. S1. Alleles from the *Iro* complex and *delta* genetically interact with *dmiR-1.*

Photographs of representative wings from matings of noted deficiencies, and alleles of *ara, caup, mirr*, and *delta* with the *dpp-GAL4::UAS-dmiR-1* fly line as discussed in Fig. 2. Parental mutant (left) or progeny with “no change” (center) or “enhanced” (right) with percentages as noted.

Supplementary Figure 2, related to Figure 1:

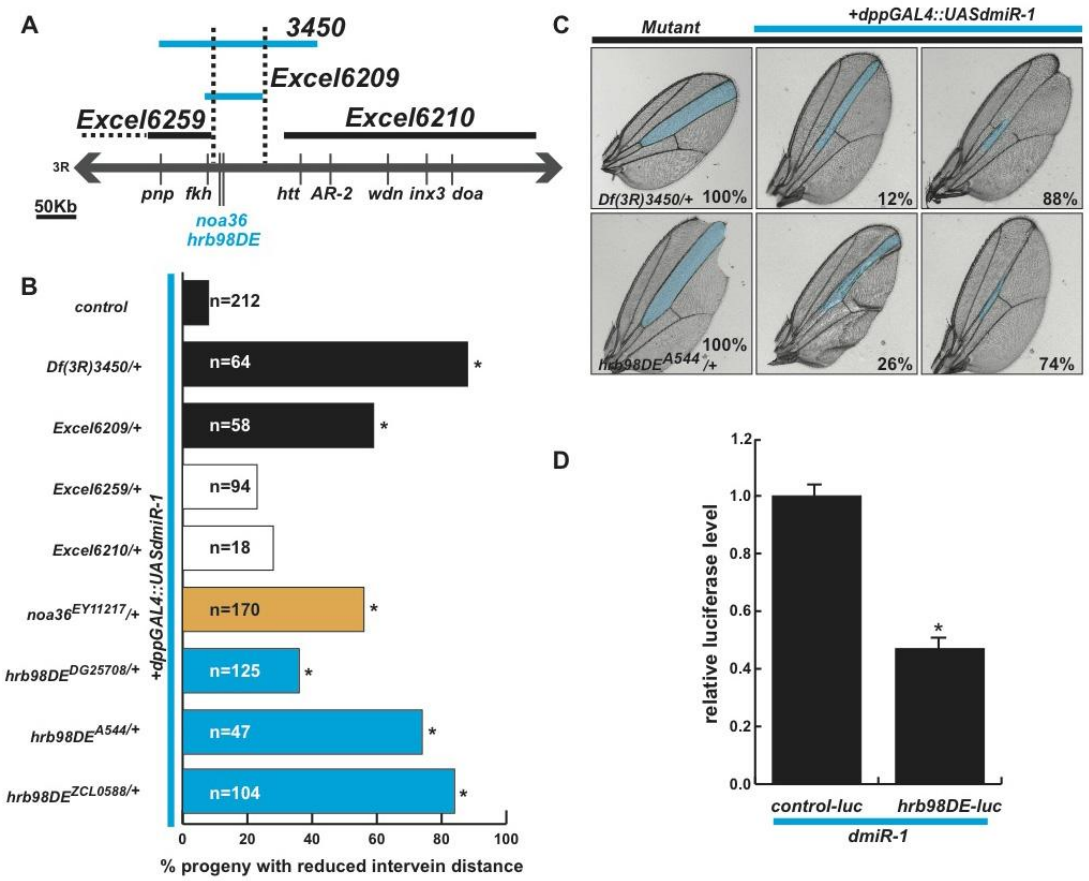

Fig. S2. *Hrb98DE* and *Noa36* genetically interact with *dmiR-1.*

(A) Schematic of the deficiencies Df(3R)*3450* and *Excel6209* spanning the genes *noa36* and *hrb98DE* that genetically enhanced the *dpp-GAL4::UAS-dmiR-1* phenotype.

(B) Graph of affected progeny per genotype as marked. n= number of offspring scored per genotype. *p<0.001. Error bars are represented as standard error of the mean.

(C) Images of representative wings of an informative deficiency line, or *hrb98DEA*^{544} mutant allele. Parental mutant (left) or progeny with “no change” (center) or “enhanced” (right) with percentages as noted.

(D) Relative luciferase activity with or without the 3′UTR of *hrb98DE* which is inserted into the 3′UTR of a constitutively active luciferase vector in the presence or absence of *dmiR-1*. *p<0.05.

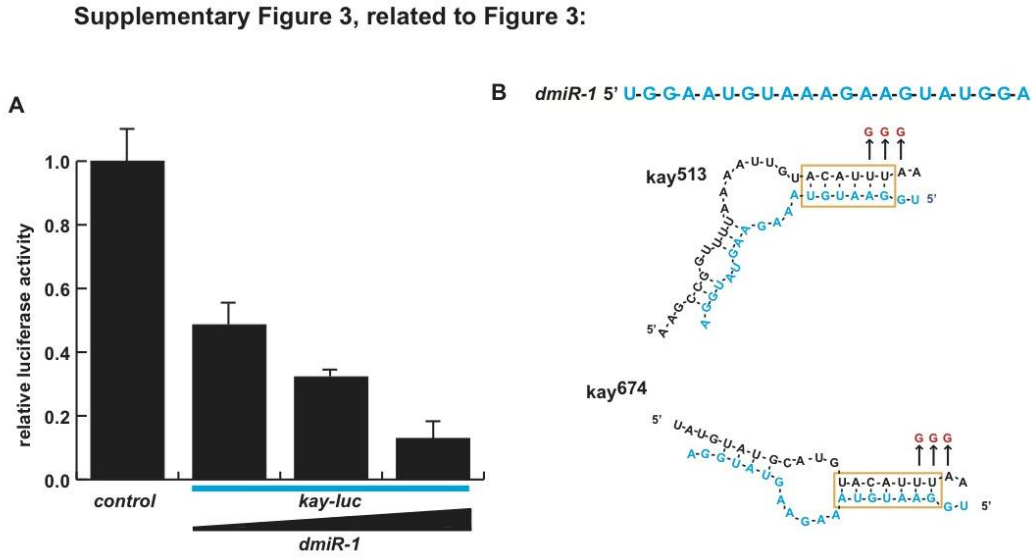

Fig. S3. *Kay* is sensitive to *dmiR-1* regulation.

(A) Relative luciferase activity with or without the 3′UTR of *kay* inserted into the 3′UTR of a constitutively active luciferase vector in the presence of 200ng, 400ng or 600ng *dmiR-1* mimic. Error bars are represented as standard error of the mean.

(B) The sequence of dmiR-1 is shown at the top, with the predicted alignment of mRNA-miRNA complex at nucleotide 513 and 674 in the 3'UTR of *kay*. Putative seed sequence is boxed in yellow and mutated residues are indicated in red. Based on the structure obtained using mfold (http://mfold.bioinfo.rpi.edu/).

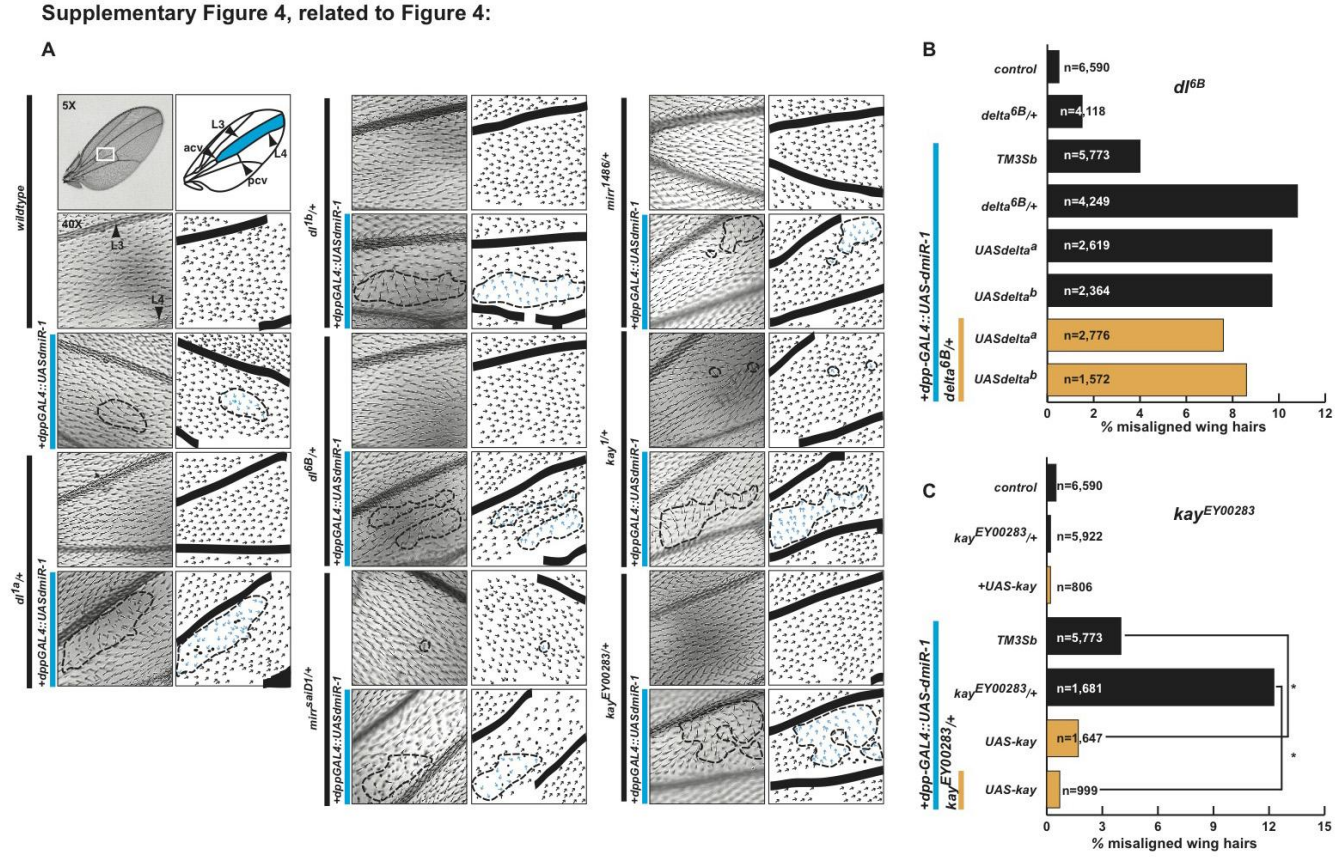

Fig. S4. Haploinsufficiency of *delta, mirror* and *kayak* increase the incidence of PCP defects in *dppGAL4::UASdmiR-1* flies.

(A) Images of representative wing tissue between L3 and L4, with genotype as noted. Schematic of photograph lies to right. White box indicates anatomical location of wing hair alignment determination. Individual hairs that are not oriented in the normal proximal to distal orientation are highlighted in blue.

(B) Concomitant expression of *UAS-Dl* and *dpp-GAL4-UASdmiR-1::Dl*$^{6B/+}$ does not rescue the wing hair phenotype. Two *UAS-delta* lines were tested (*UAS-Dl*^{a,b}). Note that both loss- and gain-of-*Dl* function resulted in mis-alignment of wing hairs. TM3Sb: control balancer.

(C) Concomitant expression of *UAS-kay* and *dpp-GAL4-UASdmiR-1::kay*^{EY00283} resulted in a rescue of wing hair misalignment. Results are representative of those seen with *kay*^{1} or *kay*^{sro} mutants. *p<0.001. TM3Sb: control balancer.

Supplementary Figure 5, related to Figure 4:

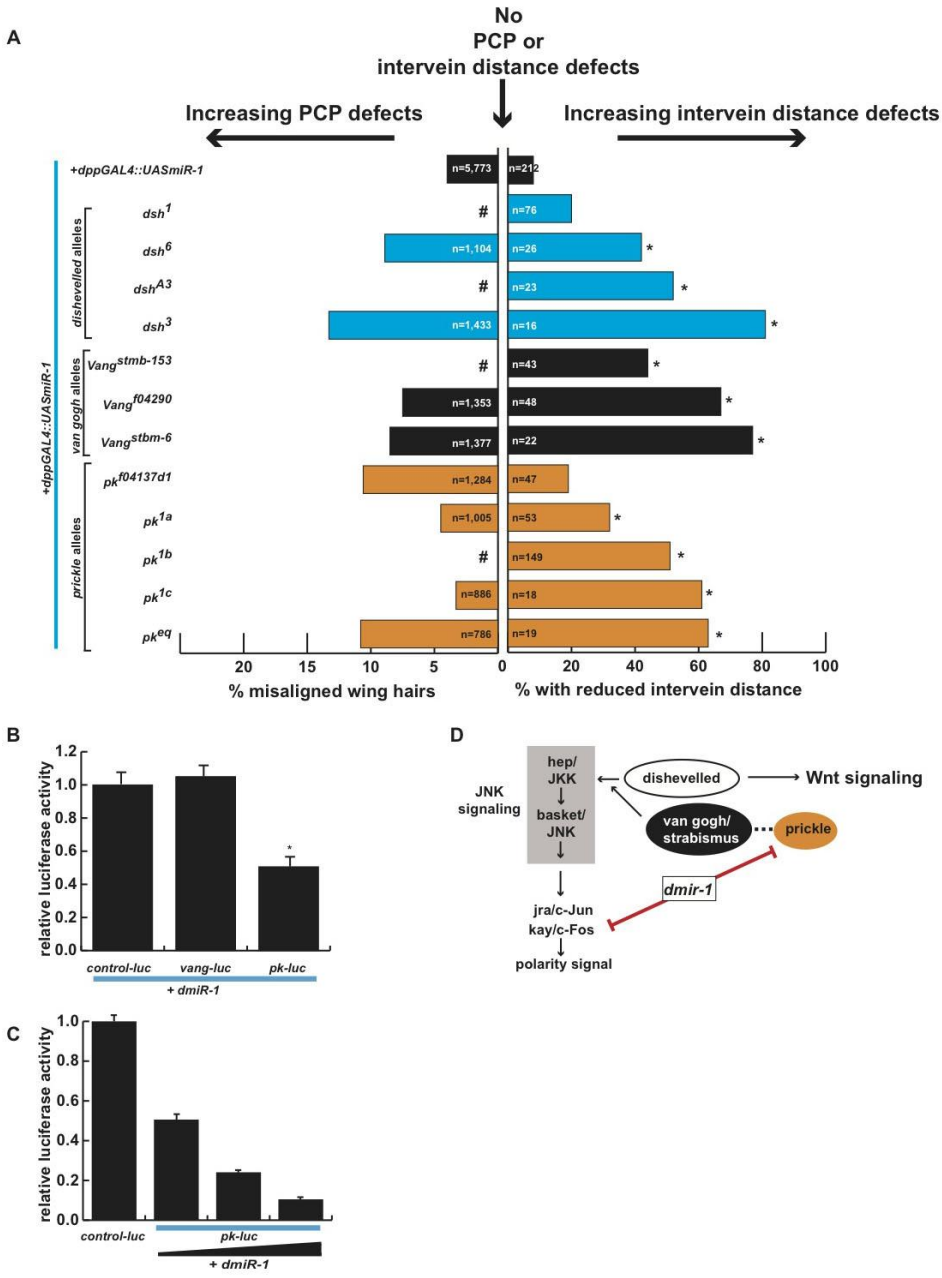

Fig. S5. *dmiR-1* genetically interacts with members of the core PCP pathway.

(A) Consequences of *dishevelled, (dsh), van gogh* (*vang*) or *prickle* (*pk*) alleles crossed to *dpp-GAL4::UAS-dmiR-1* flies. Alleles of each gene are listed, with n values representing number of wing hairs counted (left) or number of pertinent progeny scored (right). #: not interpretable, as parental line has misaligned hairs.

(B) Luciferase assay. *vang* is an indirect target, and *pk* is a direct target of *dmiR-1*. *p<0.001. Error bars are represented as standard error of the mean.

C) Relative luciferase activity with or without the 3′UTR of *pk* inserted into the 3′UTR of a constitutively active luciferase vector in the presence of 200ng, 400ng or 600ng *dmiR-1* mimic. Error bars are represented as standard error of the mean.

(D) Model of *dmiR-1* action on selected PCP proteins and its relationship to JNK signaling, kay/c-Fos, and prickle.

Supplementary Figure 6, related to Figure 5:

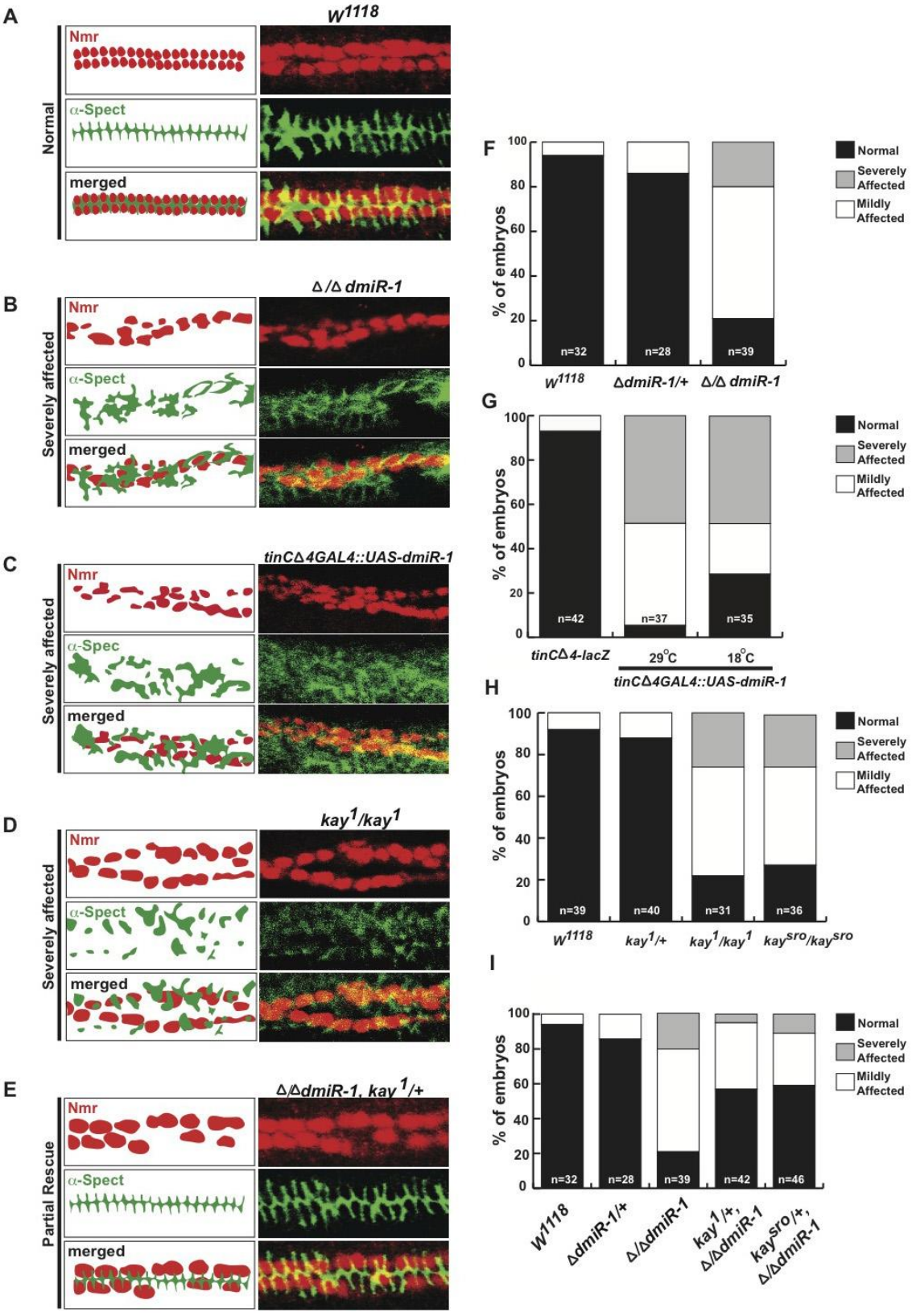

Fig. S6. Apical-basal cell polarity in the *Drosophila* heart is influenced by *dmiR-1.*

(A) Schematic of the expression pattern for Neuromancer (Nmr, red) and α-Spectrin (green) in wildtype (W^{1118}) *Drosophila* hearts (left). Confocal images showing Nmr and α-Spectrin localization within the fly heart in wildtype (W^{1118}) stage 16 embryos (right).

(B) Schematic (left) and confocal (right) images of homozygous-null *dmiR-1* stage 16 embryos, with Nmr and α-Spectrin expression in red and green, respectively.

(C) Schematic (left) and confocal (right) images of *tinC Δ4GAL4::UASdmiR-1* stage 16 embryos, with Nmr and α-Spectrin expression in red and green, respectively.

(D) Schematic (left) and confocal (right) images of homozygous mutant kay^{1} stage 16 embryos, with Nmr and α-Spectrin expression in red and green, respectively.

(E) Schematic (left) and confocal (right) images of homozygous-null *dmiR-1*, kay^{1}/+ stage 16 embryos, with Nmr and α-Spectrin expression in red and green, respectively.

(F) Quantification of panel (B) with normal (black), mildly (white), or severely (grey) affected embryos, according to genotype. Scoring was based on the degree of mis-alignment of the cardioblasts and diffuse expression of α-Spectrin.

(G) Quantification of panel (C) with normal (black), mildly (white), or severely (grey) affected embryos, according to genotype and temperature.

(H) Quantification of panel (D) with normal (black), mildly (white), or severely (grey) affected embryos, according to genotype.

(I) Quantification of panel (E) with normal (black), mildly (white), or severely (grey) affected embryos, according to genotype.

Supplementary Figure 7, related to Figure 5:

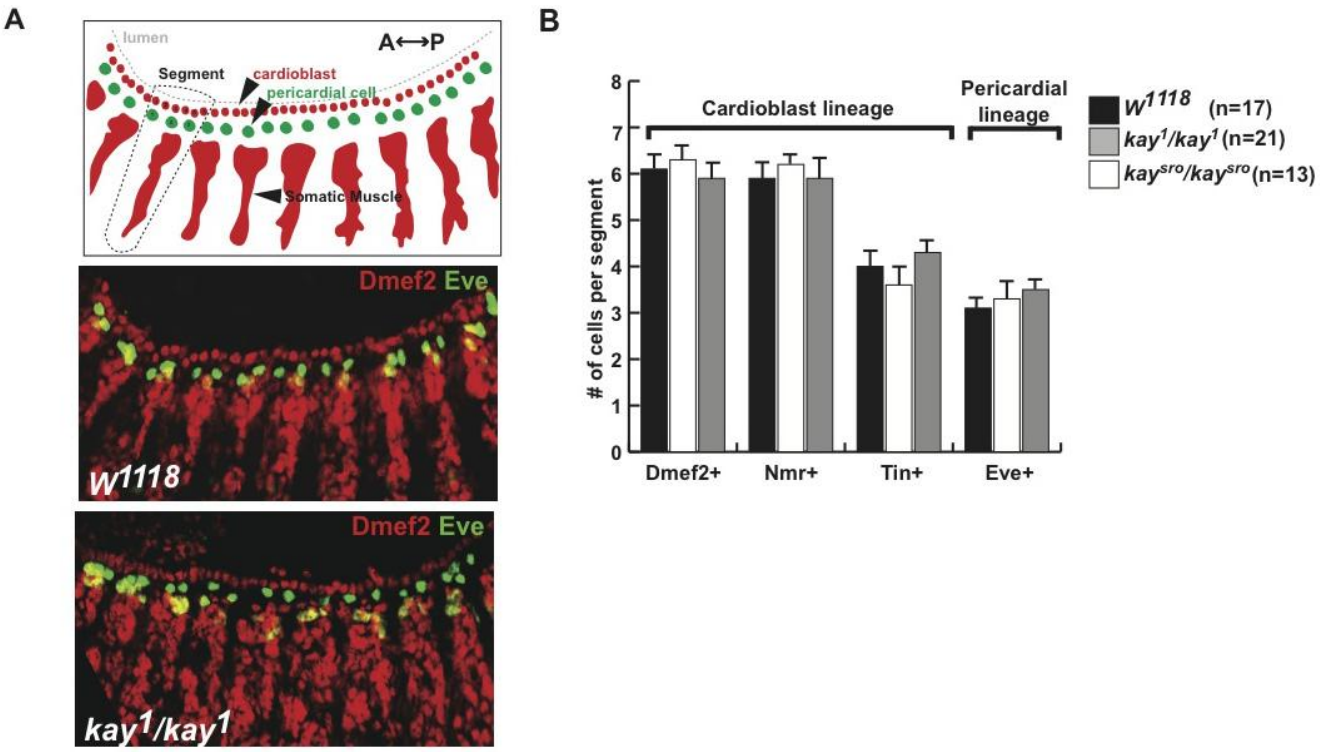

Fig. S7. The cardioblasts and pericardial cells of stage 16 *kay* null embryos are correctly specified.

(A) Schematic of a lateral view of a stage 14 *Drosophila* embryo with the pertinent cardiac structures labeled (top) and the corresponding confocal views of wildtype (W^{1118}) or homozygous kay^{1} mutants (middle, bottom). Red, DMef2; green, even-skipped (Eve) immunostaining.

(B) Comparison of numbers of cells of the cardioblast and epicardial lineage in embryos homozygous for *kay alleles* compared to wild type. Error bars are represented as standard error of the mean.

Supplementary Figure 8, related to Figure 6:

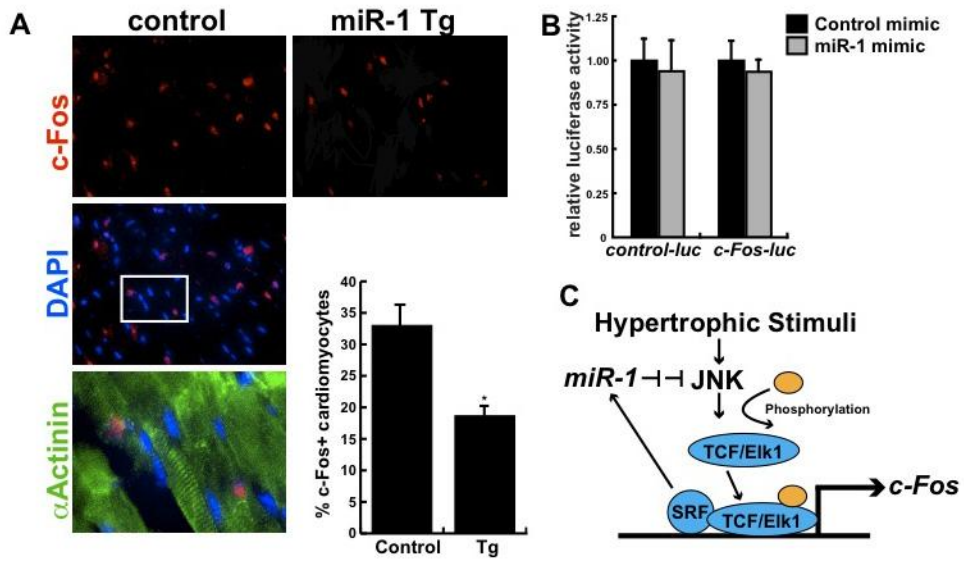

Fig S8. *c-Fos* expression in murine heart is limited to cardiomyocytes, and is indirectly regulated by *miR-1*.

A) Immunohistochemistry of murine heart sections in wild type and transgenic animals stained with anti-c-Fos antibodies (red). Cardiomyocytes were labeled with anti-α-actinin antibodies (green) and nuclei stained with DAPI (blue). Bottom Left: enlarged view of area highlighted in white box. Bottom Right: Quantification of cells positive for c-Fos and α-actinin in wildtype or α-MHC-miR-1 transgenic (Tg) hearts. *p<0.05. Error bars are represented as standard error of the mean.

B) Luciferase activity with the *c-Fos* 3'-UTR inserted downstream of a luciferase reporter in the presence or absence of miR-1. Error bars are represented as standard error of the mean.

C) Potential model of indirect miR-1 regulation of c-Fos through the regulation of JNK signaling.

Table 1. Results of tested deficiencies by chromosome. (see Excel file)